



LB - 844

THE PLASMATRON, A CONTINUOUSLY-

CONTROLLABLE GAS-DISCHARGE

DEVELOPMENTAL TUBE

**RADIO CORPORATION OF AMERICA
RCA LABORATORIES DIVISION
INDUSTRY SERVICE LABORATORY**

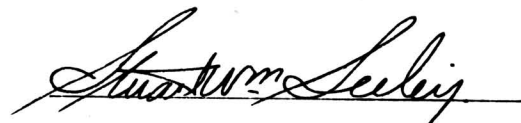
RADIO CORPORATION OF AMERICA
RCA LABORATORIES DIVISION
INDUSTRY SERVICE LABORATORY

LB-844

The Plasmatron, a Continuously-Controllable
Gas-Discharge Developmental Tube

This report is the property of the Radio Corporation of America and is loaned for confidential use with the understanding that it will not be published in any manner, in whole or in part. The statements and data included herein are based upon information and measurements which we believe accurate and reliable. No responsibility is assumed for the application or interpretation of such statements or data or for any infringement of patent or other rights of third parties which may result from the use of circuits, systems and processes described or referred to herein or in any previous reports or bulletins or in any written or oral discussions supplementary thereto.

Approved



The Plasmatron, a Continuously-Controllable Gas-Discharge Developmental Tube

Introduction

This bulletin describes and analyzes the operation of the "plasmatron", a new type of continuously controllable gas-discharge tube. This tube utilizes an independently generated gas-discharge plasma as a conductor between a hot cathode and an anode. Continuous modulation of the anode current can be effected either by variation of the conductivity or the effective cross section of the plasma. The first of these is accomplished by the modulation of the electron ionizing beam which controls the plasma density and hence its conductivity. The second method makes use of the gating action of positive ion sheaths which surround the wires of a grid located between the anode and cathode. The plasmatron appears to have considerable promise for such applications as motor drive, direct loud-speaker drive, high-efficiency rectification and inversion, and the many other uses which require the high-current and low-voltage operation that the high-impedance vacuum tube cannot supply.

General Discussion

As a consequence of its space-charge-limited current the vacuum tube is a relatively high-impedance device. It is a most useful device because the current through it can be continuously controlled. On the other hand, a gas tube such as the thyratron, which normally operates with a neutralized space charge, is a low-impedance device. Unfortunately, it seems that it has been necessary to pay a large price for this low-impedance operation. The enormous advantage of continuous current control has been lost.

However, the situation is far from hopeless. In fact, if one approaches the operation of hot-cathode gas tubes in terms of new concepts based on the fundamental processes, it appears that it is entirely possible and practicable to have both low-impedance operation and the continuous control in one tube. The plasmatron is such a tube. It can deliver, and continuously control, large currents at anode potentials of a few volts. This tube, now in

the developmental stage, shows excellent promise of fulfilling the long-standing need for a tube that will continuously control large currents at low voltages. In this category are found such applications as motor control, direct loudspeaker drive, inverters, and the like.

The name "plasmatron" stems from the word "plasma"¹ which denotes an important part of a gas discharge. The plasma is a region of very high, but essentially equal, concentrations of free electrons and ions. Due to the high mobility of the plasma electrons and the absence

¹L. B. Loeb, FUNDAMENTAL PROCESSES OF ELECTRICAL DISCHARGES IN GASES, John Wiley and Sons, New York, N.Y., 1939.

J. D. Cobine, GASEOUS CONDUCTORS, McGraw-Hill, New York, N. Y., 1941.

Rompe and Steenbeck, "The Plasma State of Gases", *Ergeb. exakt., Naturw.*, Vol. 18, pp. 257-376; 1939. Translated from the German by G. C. Akerlof, Mellen Inst. of Industrial Research.

of net space charge, the plasma is a rather good electrical conductor. It has a resistivity of the order of one ohm centimeter which places it in a class with semiconductors such as germanium. As a consequence of this high conductivity, the electric fields within the plasma are small.

The principle of operation of the plasmatron lies in the use of a plasma as a conductor between a hot cathode and an anode. This plasma, however, is generated by an auxiliary discharge (which operates independently of the work circuit) and *not* by the anode current as is the case with a thyatron. It will be seen that this seemingly small difference is of fundamental importance.

There are two broadly different methods of effecting continuous control over the anode current. The first makes use of the fact that the conductivity of plasma, and hence the anode current, depends upon the plasma density and this, in turn, upon the intensity of the auxiliary discharge which generates the plasma. The second method involves the use of a grid structure that is interposed between the cathode and the anode. This grid, by virtue of the positive ion sheaths that surround it, gives a gating action that acts to control the effective cross-section area of the plasma conductor and hence the current carrying capacity of the tube.

Briefly, the reason that the plasmatron grid can effect continuous control over the anode current, whereas the thyatron grid commonly cannot, lies in the fact that the ion generation in the plasmatron is achieved by an independent discharge and not by the anode current itself. It is also pertinent to point out that in a thyatron the applied anode potential really serves a double function: (1) to provide electrons with enough energy to generate ions, and (2) to provide the electric field needed for pulling the required anode current through the tube. When these functions are separated, as they are in the plasmatron, it is found that the potential needed for drawing a given anode current is greatly reduced and, in addition, continuous grid control becomes possible, provided that the anode potential is insufficient to cause ionization.

Rather than starting with a detailed exposition of the operation of the tube, it seems expedient that the first part of the

paper be concerned with the building up of a general picture of the overall operation and characteristics of the tube. This picture will then provide a convenient point of departure for the remainder of the paper wherein the operation is treated in more detail. With this approach in mind, it is now convenient to consider the first mode of modulation or control.

Diode Operation*

Fig. 1 shows an experimental form of plasmatron designed for and operating in the diode mode. The plasmatron is seen to consist of a main anode in the shape of an inverted U; two cathodes, one referred to as the main, and the other as the auxiliary cathode; and a cylinder with a narrow aperture, this cylinder being designated as the garrote. Fig. 2 is a photograph of a tube of the form sketched in Fig. 1. While it has been found convenient to

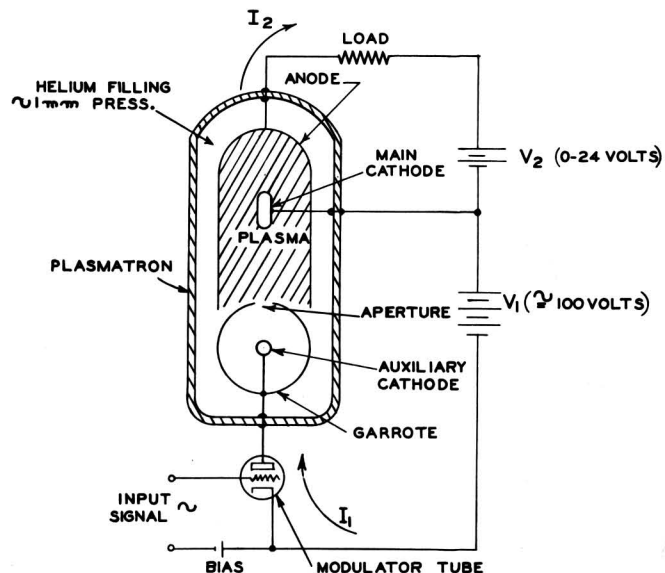


Fig. 1 - Circuit arrangement for diode operation.

work with experimental tubes of the form shown in Fig. 2, the principle of operation puts no definite restrictions upon the size or geometry of the tube provided the basic features are retained. The circuit is seen to consist of two loops referred to as the main loop and auxiliary

*E. O. Johnson, "Controllable Gas Diode", *Electronics* Vol. 24, pp. 107-109; May, 1951.

loop, respectively. Most experimental tubes are filled with helium to a pressure of one millimeter of mercury.

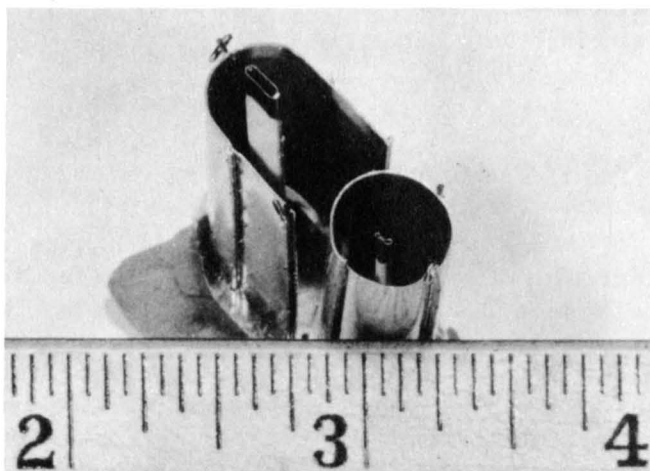


Fig. 2 - Photograph of typical plasmatron diode.

In operation V_1 is made sufficiently large so that a discharge occurs in the auxiliary loop, current flowing between the auxiliary cathode and the upper portion of the structure. This discharge generates a plasma between the main cathode and anode enabling large currents to flow between them for small values of V_2 . In fact, as will be seen, in order to insure plasmatron operation V_2 must be held below a value which would initiate a discharge in the main loop. The garrote (generally tied to the auxiliary cathode) serves to achieve the generation of a dense plasma for small discharge currents. It increases the ionization efficiency to such an extent that several milliamperes in the auxiliary circuit enables hundreds of milliamperes to flow in the main or work circuit.

In the circuit, as shown, the auxiliary discharge current can be varied by means of changes in the grid potential of the modulator tube, which in this case is a small vacuum tube such as the 6J5.

A typical volt-ampere characteristic, with the auxiliary discharge current as parameter, is shown in Fig. 3. It is seen that the anode current starts to flow when the anode is about minus one volt, rises rapidly, and finally saturates at a current of over half an ampere (for $I_1 = 8$ milliamperes) when the anode potential is only about 3 volts. The current remains saturated along this curve until the

anode potential exceeds about 25 volts, the ionization potential of helium, and then rises steeply without regard to the value of the auxiliary current. In practice, the tube is always operated below this break point. In fact, for normal operation a load line should be fitted in between the saturation voltage and the ionization voltage. The back current for negative anode potentials is of the order of a few milliamperes and consists of positive ion current from the plasma. For negative anode potentials greater than about 200 volts, in the tube illustrated, a cold discharge will take place between the anode surface and the cathode.

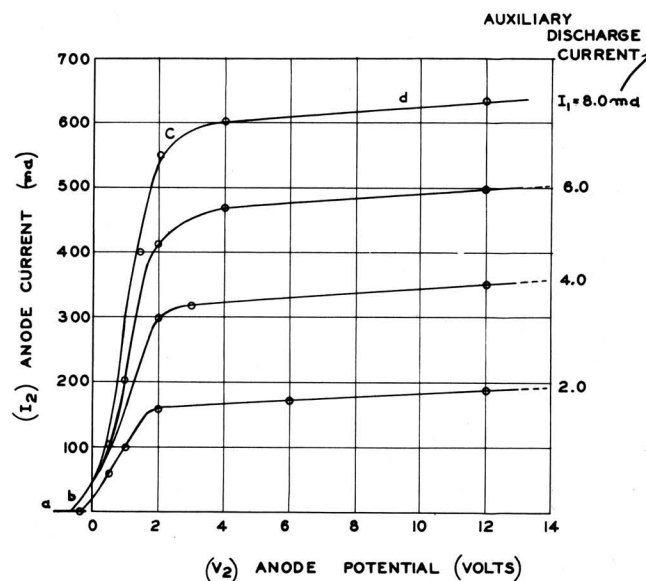


Fig. 3 - Diode volt-ampere characteristic.

Fig. 4 shows the relationship between the auxiliary current and the saturated main current. The relation is seen to be a linear one until the main current exceeds about one ampere. The departure from linearity beyond here arises from the onset of emission saturation of the main cathode. When the cathode is completely saturated the anode current becomes equal to the value of this current since the plasmatron, like any other electron tube, is limited in peak anode current to the saturated cathode emission. Whereas the current gain is only about 100:1, as exemplified by the slope at low currents, improved tubes give gains of 300 or better. The power gain for this tube is about 17 decibels.

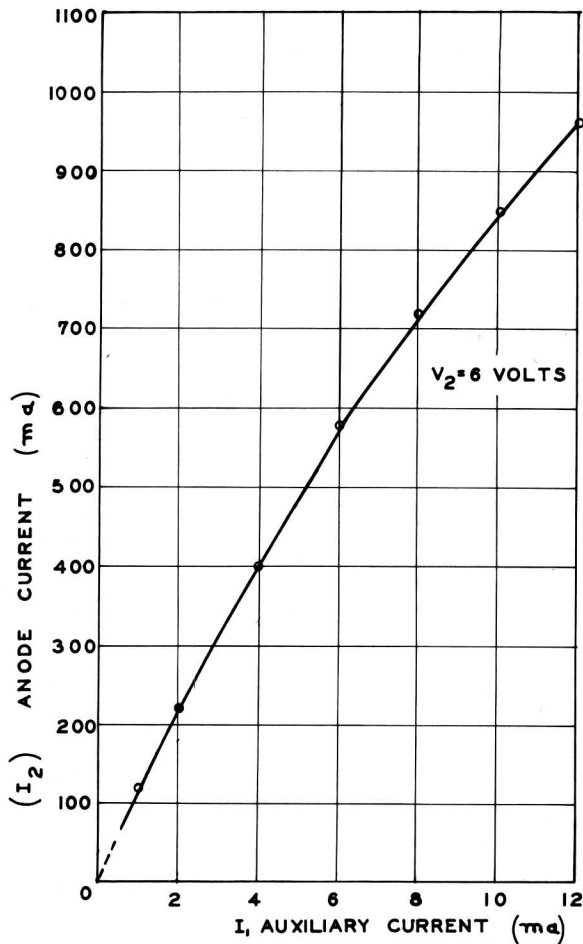


Fig. 4 - Diode control characteristic.

The frequency response is shown in Fig. 5. The current gain is seen to be flat from dc out to about 10 kilocycles and then fall off. This falling off with frequency arises from the length of time required for surplus ionization to diffuse away to the end micas where surface recombination of the free electrons and positive ions takes place. For helium at these gas pressures and for these tube sizes the volume

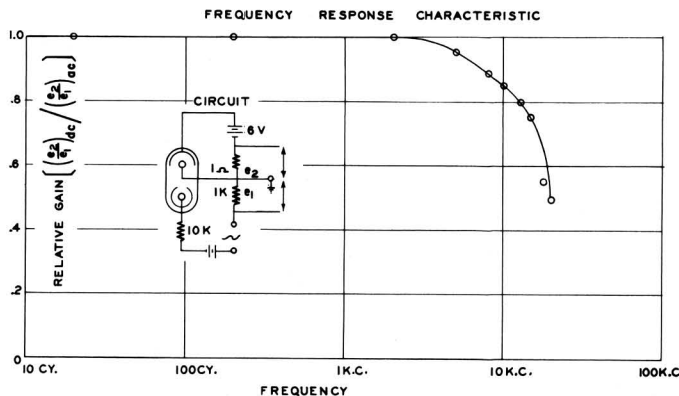


Fig. 5 - Diode frequency characteristic.

recombination of the particles in the plasma is relatively small. As will be shown later the unique potential distribution between the cathode and anode prohibits positive ions from reaching these surfaces.

Triode Operation

The arrangement for the second mode of control employing a grid located between the cathode and anode is shown in Fig. 6. The circuit is seen to be almost identical with the diode circuit except that the modulator tube has been replaced with a limiting resistor and,

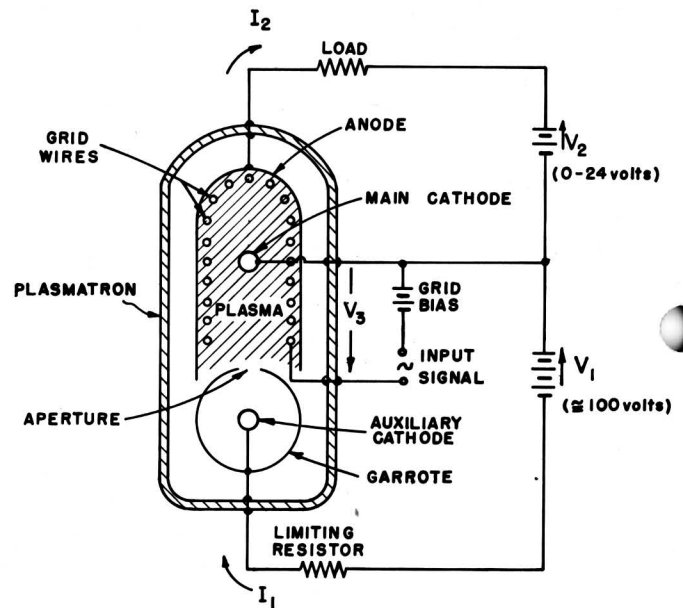


Fig. 6 - Circuit arrangement for triode operation.

in addition, a grid circuit has been added. A photograph of a typical experimental triode plasmatron, with its anode folded back to allow a view of the grid structure, is shown in Fig. 7.

The mechanism of grid control is depicted in Fig. 8 where a section of the anode and two of the grid wires are shown. The cathode is out in the plasma towards the bottom of the figure and need not concern us. As was pointed out previously, the plasma has a high conductivity so that the electric fields within it are always small. External fields are absorbed at the plasma boundaries in a thin layer called sheath.¹ This is illustrated in the potential

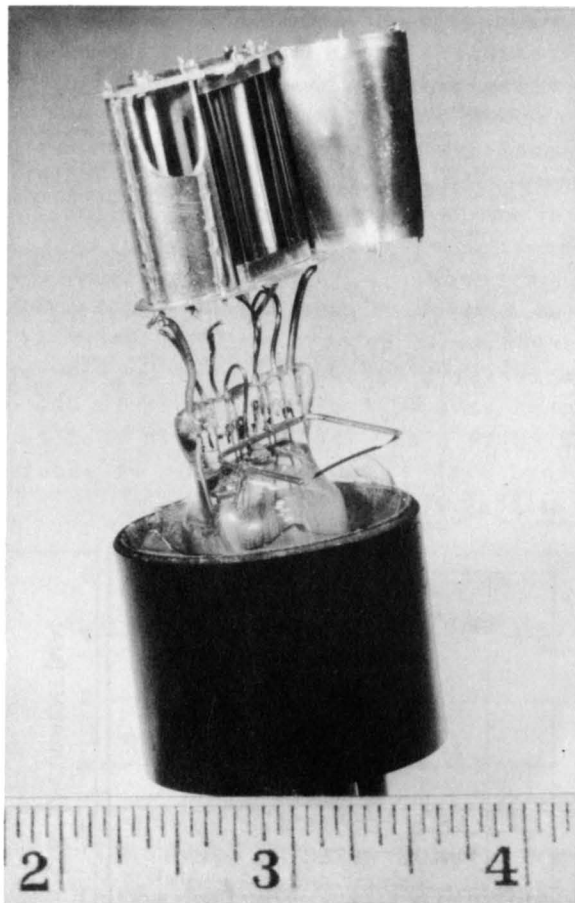


Fig. 7 - Photograph of typical plasmatron triode.

diagram which is a projection of the cross section above. The sheath, which is the transition between the plasma and the grid wire, is nothing more than a region containing positive ions enroute to the grid wire. It is the plasma's way of meeting its boundary conditions. One can picture the edge of the plasma as being a positive ion emitter and the grid wire as being the collector. The thickness of the sheath is determined by the positive ion current and the grid voltage according to the familiar $3/2$ power law.¹ Since the ion current is a constant, being set by the rate at which ions diffuse out of the plasma, the sheath thickness will increase with the negative grid voltage until adjacent sheaths overlap. The negative field in the sheaths will repel the electrons which would otherwise go to the anode, and the anode current is then cut off. Intermediate anode currents result from sheaths of intermediate radii.

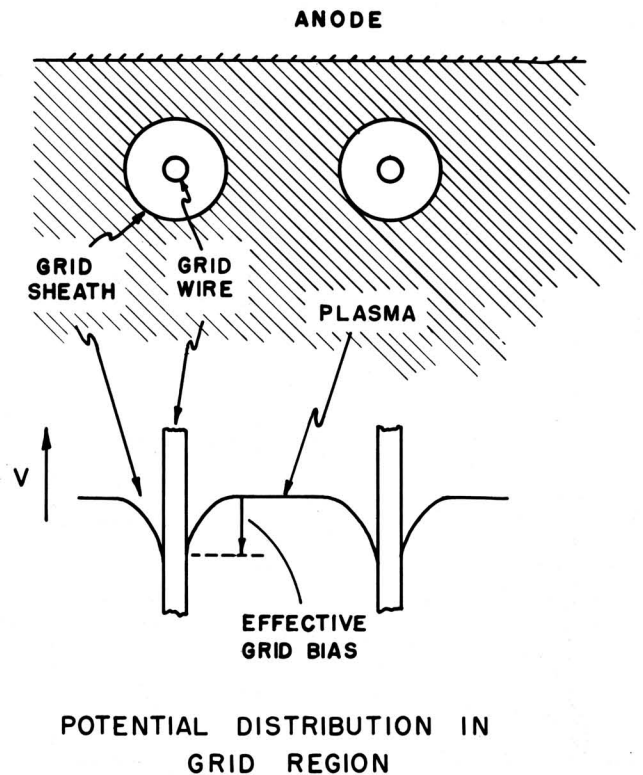


Fig. 8 - Diagram illustrating grid action.

The volt-ampere characteristic with the grid bias as parameter is shown in Fig. 9. The auxiliary current is held constant. It is seen that this family of curves is similar to those in Fig. 3. This similarity stems from the fact that variations in the plasma cross-section area turn out to be effectively equivalent to variations in the plasma conductivity. As in the diode the load line should be placed between the saturation and the ionization voltages. However, if the grid cuts off the anode current before the anode potential exceeds the ionization potential then the anode potential can be permitted to exceed the ionization potential without re-establishing the flow of anode current. But, just as with a thyatron, if anode current flow starts at elevated anode potentials the grid loses control.

Fig. 10, which is a replot of the data shown in Fig. 9 for a constant anode voltage, shows that the grid characteristic is a non-linear one. Whereas the transconductance exceeds 100,000 micromhos at low grid voltages it drops below 10,000 for biases greater than about 6 volts.

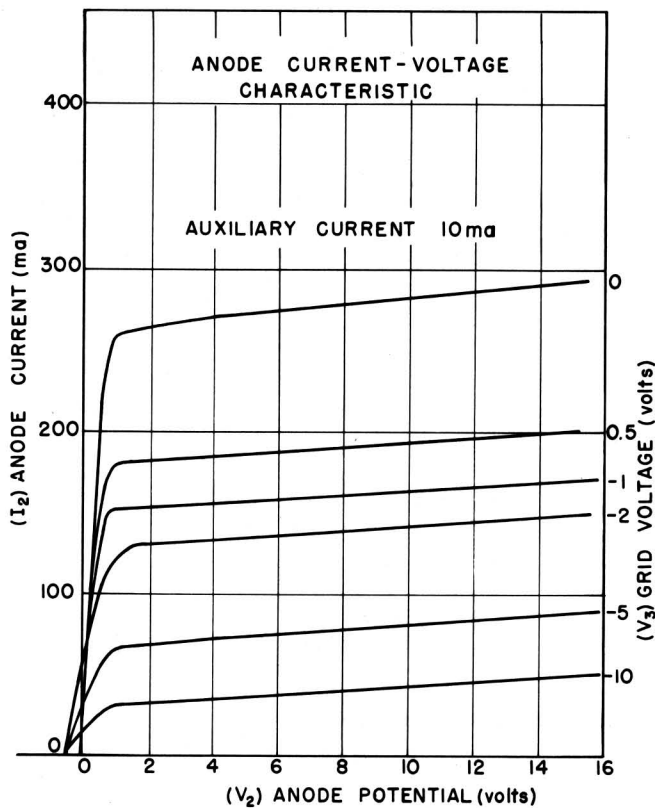


Fig. 9 - Triode voltampere characteristic.

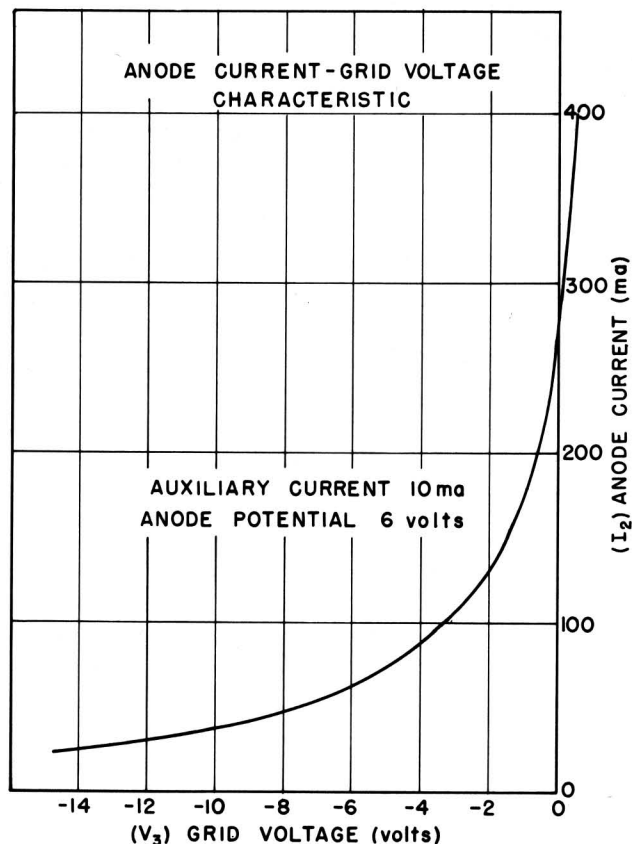


Fig. 10 - Triode control characteristic.

The current-voltage characteristic of the grid is shown in Fig. 11. For negative grid potentials greater than about 1.5 volts the grid current is predominately ionic, while for more positive potentials the electrons predominate. The very rapid rise in the electron current which occurs at low grid voltages is a consequence of the grid's beginning to act like an anode. In fact, if the curves were carried further, a characteristic like that of the anode would be obtained. The slope of the characteristic is seen to vary between about 300 ohms at 1 volt bias to about 10,000 ohms at 10 volts bias. The power gain that can be obtained with triode operation is about the same as that with diode operation.

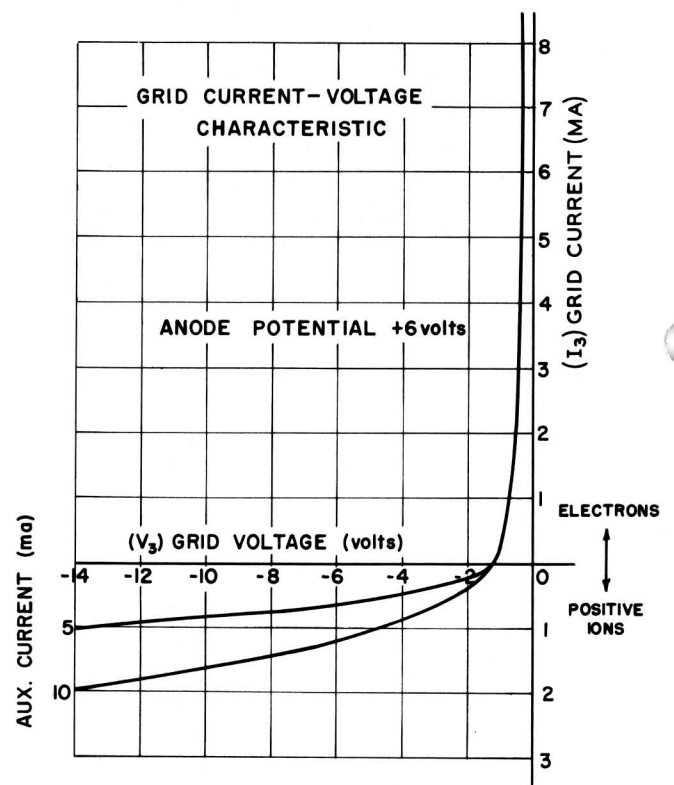


Fig. 11 - Grid voltampere characteristic.

A typical frequency response of a grid-controlled tube is displayed in Fig. 12. Since grid modulation affects the plasma only in a small region adjacent to the grid, whereas the diode modulation requires bulk changes in the plasma, it is not surprising that the triode frequency response is a markedly better one. The wiggles in the triode response result from a complex combination of ion and electron movements which accompany the propagation and retraction of the grid sheath. The response was

not studied beyond 10 Mc other than observing that a tube could operate as a class C oscillator at frequencies as high as 17 Mc.

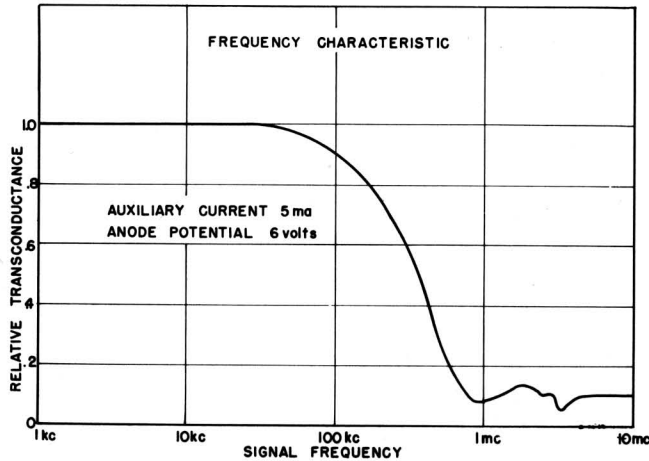


Fig. 12 - Triode frequency characteristic.

Plasma Characteristic¹

The plasma in a gas discharge can often be identified with the region that shows a visible glow. Whereas the glow itself arises from excitation of the gas atoms, the excitation in most gas-discharge devices is almost sure to be accompanied by the dense ionization that characterizes a plasma. This is the case in the plasmatron. The density of the free electrons and positive ions which constitute the plasma in experimental or commercial gas-discharge tubes ranges from 10^9 to about 10^{11} particles per cm.³ Since there are essentially equal densities of the oppositely charged particles the plasma is electrically neutral. In a typical plasma the charged particles usually execute random motions conforming to a Maxwellian distribution of velocities. It is then convenient to describe these motions in terms of a temperature. In the cases to be described it will be assumed that the positive-ion temperatures are about the same as the ambient-gas temperature. This seems reasonable because of the high collision frequency between the ions and neutral atoms at the pressures in the tubes to be described. The electrons, in most cases, have a much higher temperature.

The high density of the electrons along with their high mobility in a region largely

devoid of space charge makes possible the conduction of large electron currents for very low applied potentials. The conductivity of a uniformly dense plasma which is electrically neutral is given by

$$\sigma = Ne\mu \text{ mhos per centimeter} \quad (1)$$

where N is the electron density per cubic centimeter, e is the electron charge in coulombs, and μ is the electron mobility in centimeters per second per volt per centimeter. For a typical plasma $N = 5 \times 10^{10}$ and $\mu = 5 \times 10^6 \frac{\text{cm}}{\text{sec}} / \frac{\text{volt}}{\text{cm}}$. Thus σ is 4.0×10^{-2} mhos per cm which is comparable with the conductivity of a semiconductor like germanium.

From kinetic theory, it is found that the electron space-current density is given by

$$j_e = \frac{1}{4} Ne\bar{c} \quad (2)$$

where \bar{c} , which is the average thermal velocity of the electrons, is given by:

$$\bar{c} = 1.87 \times 10^{-8} \sqrt{\frac{T_e}{m}} \quad (2')$$

T_e is the electron temperature and m the electron mass. Choosing as typical values $N = 5 \times 10^{10}/\text{cm}^3$, $\bar{c} = 2 \times 10^7 \text{ cm/sec}$, and $T_e = 1000^\circ \text{ K}$, it turns out that $j_e = 40 \text{ ma/cm}^2$. A similar computation for the positive ion space-current density yields (for helium) $j_p = 0.27 \text{ ma/cm}^2$.

The transition between a plasma and a bounding electrode or wall occurs in a thin region of space charge which is termed a sheath. It is in the sheath that the fields from electrodes are dissipated, leaving the plasma essentially unaffected by electrode or wall potentials. If the electrode is negative with respect to the plasma, electrons are repelled from the sheath leaving only a current of positive ions flowing to the electrode. The thickness of this layer of moving positive ions adjusts itself so that the electric flux from the electrode ends on the moving charges. Accordingly the sheath thickness d in centimeters can be related to the potential V in volts, and to the positive ion current density

j_p in amperes per square centimeters by the familiar Child-Langmuir space-charge law (for plane structures):

$$j_p = \frac{2.33 \times 10^{-6}}{\sqrt{\frac{M}{m}}} \frac{V^{3/2}}{d^2} \quad (3)$$

where M is the ion mass and m the electron mass. If the electrode is positive with respect to the plasma the sheath will contain a space charge of electrons. The current density j is fixed by conditions within the plasma and is given by Eq. (2) written for the appropriate particle. The density value used in this expression must apply close to the edge of the plasma. The current value obtained by Eq. (2) is only approximately correct since no account is taken of the drift due to the weak electric fields within the plasma and at its edge. However, for purposes of simplicity this expression will be assumed to be correct.

It is now possible to consider the behavior of a cold electrode immersed in a plasma as its potential with respect to the plasma is varied. A typical current-voltage characteristic is shown in Fig. 13. Along portion ab of the characteristic all the electrons are repelled and only positive ions flow from the plasma to the electrode. The sheath thickness is given by Eq. (3) in which j_p is derived from Eq. (2).

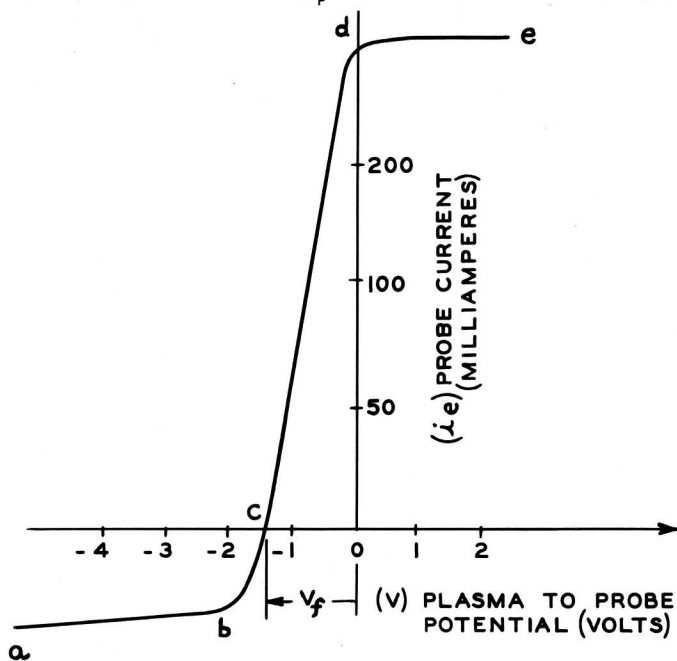


Fig. 13 - Plasma cold-electrode characteristic.

As the potential of the electrode becomes increasingly negative the current increase slightly due to sheath expansion. Beyond point b on the way to d the electron current to the electrode increases rapidly according to the Boltzmann relation

$$i_e = A_p j_e e^{\frac{eV}{kT_e}}$$

$$\phi = \frac{e}{k T_e} \quad (4)$$

where $j_e = \frac{NeC}{4}$ is the random electron space current near the edge of the plasma, A_p is the probe area, and k is the Boltzmann constant. The electron temperature T_e can be determined from the semilog plot of i_e against V for the region cd. When point d is reached the voltage V is zero and the electrode is at plasma potential where it collects the full electron space current. For convenience the magnitude of the positive ion current with respect to the electron current has been greatly exaggerated. Actually the saturated ion current, as pointed out in conjunction with Eq. (2), is smaller than the electron space current by a factor of more than a hundred. Beyond point d, as we proceed to point e, the electron current increases slowly as the electron sheath builds up according to Eq. (3).

At point c the electron and ion currents to the electrode are equal and, since this is the point at which the electrode would "float", the corresponding plasma to electrode potential V_f is called the floating potential.

Cathode-Plasma Anode System

In the preceding discussion the complete circuit was neglected for purposes of simplicity. It is apparent that in a practical system a return circuit must be provided. The simplest possible system with two cold electrodes and an independently produced plasma has been treated elsewhere.² Let us now suppose that one of the electrodes is a hot cathode with a total emis-

²E. O. Johnson and L. Malter, "A Floating Double Probe Method for Measurements in Gas Discharges," *Physical Review*, Vol. 80, pp. 58-68; October, 1950.

sion density j_k ; the other electrode is the anode. As will be seen there are two cases to consider: (1) the cathode is a relatively weak emitter such that $j_k \ll j_{ok}$, and (2) the cathode is a strong emitter such that $j_k \gg j_{ok}$. Here, j_{ok} is the random electron current density in the vicinity of the cathode; j_{oa} is the random current density in the vicinity of the anode. V_k is the plasma-cathode potential difference; V_a is the plasma-anode potential difference; V_s accounts for the potential drop through the plasma and for the contact potential difference between the cathode and anode; V_2 is the cathode-anode potential difference. These quantities are indicated in the circuit diagram of Fig. 14 and in the potential diagrams of Fig. 15.

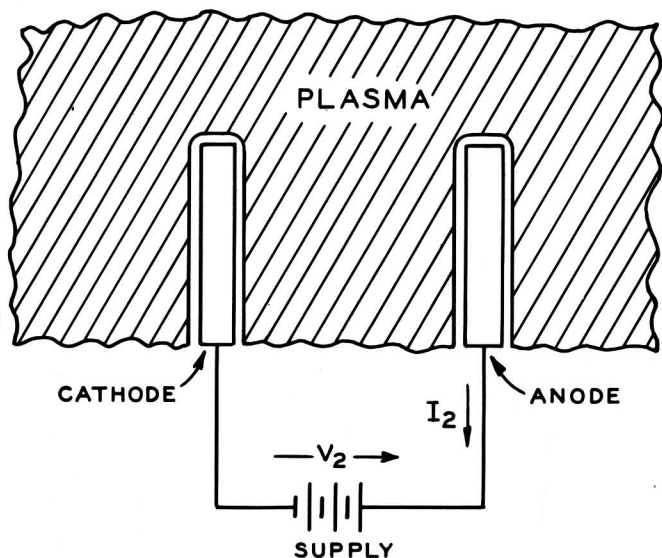
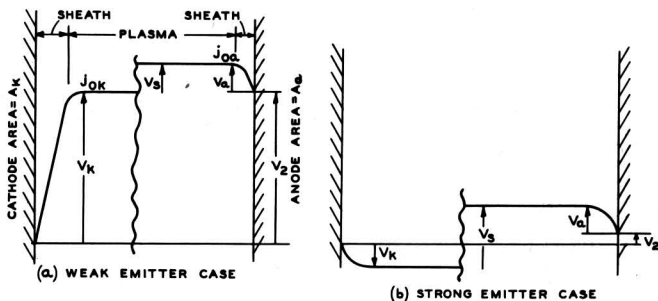


Fig. 14 - Cathode-plasma-anode system.



j_{0k} - ELECTRON SPACE CURRENT IN THE PLASMA ADJACENT TO THE CATHODE.
 j_{0a} - ELECTRON SPACE CURRENT IN THE PLASMA ADJACENT TO THE ANODE.
 V_k - CATHODE TO PLASMA POTENTIAL.
 V_s - SUM OF CONTACT POTENTIAL DIFFERENCES PLUS PLASMA DROP.
 V_a - ANODE TO PLASMA POTENTIAL.
 V_2 - CATHODE TO ANODE POTENTIAL.

Fig. 15 - Potential diagram

(a) Weak emitter case
 (b) Strong emitter case

In the first case the potential diagram is as shown in Fig. 15a. Neglecting the relatively small ion currents there will be an electron current $j_k A_k$ leaving the cathode, a current $j_{ok} A_k \exp(-\phi V_k)$ entering the cathode from the plasma, and a current $j_{oa} A_a \exp(-\phi V_a)$, which is equal to the electron current I_2 in the circuit, entering the anode from the plasma. ϕ is defined in Eq. (4). For equilibrium

$$j_k A_k = j_{ok} A_k e^{-\phi V_k} + j_{oa} A_a e^{-\phi V_a}$$

From the potential diagram

$$V_k + V_s = V_a + V_2$$

Manipulation of the preceding equations yields

$$I_2 = \frac{A_k j_k}{1 + \left[\frac{A_k j_{ok}}{A_a j_{oa}} e^{\phi V_s} \right] e^{-\phi V_2}} \quad (5)$$

While experimental studies show the essential correctness of Eq. (5), the fact that it represents a mode of operation that is not used in the plasmatron impels us to proceed at once to the second case.

With the cathode acting as a very strong emitter a retarding field must be present at its surface to limit the net current leaving. In this case the potential distribution is as shown in Fig. 15b. One can, as before, equate the electron current leaving the electrodes to that arriving. Thus,

$$A_k j_k e^{-\phi V_k} = A_k j_{ok} + A_a j_{oa} e^{-\phi V_a},$$

$$I_2 = A_a j_{oa} e^{-\phi V_a}, \text{ and } V_k + V_2 + V_a = V_s$$

The solution of these equations is

$$I_2 = \frac{A_k j_{ok}}{2} \left[\sqrt{1 \pm 4 \left(\frac{A_a j_k}{A_k j_{ok}} \frac{j_{oa}}{j_{ok}} e^{-\phi V_s} \right) e^{\phi V_2}} - 1 \right] \quad (6)$$

The electron sheath at the cathode is so thin

compared to the usual cathode radius that the area of this sheath has been replaced with that of the cathode. Also, in this simple derivation, we have neglected any changes in the potential across the plasma as well as changes in the plasma density.*

In Fig. 16 the anode current as determined by Eq. (6) is compared with experiment. The plasmatrons used in these experiments were of about the same overall dimensions and geometry as the one illustrated in Figs. 1 and 2 except that a more symmetrical (cylinder of 2-cm diameter) anode structure was employed. In addition, two 10-mil wire probes were mounted parallel with the cathode, one close to the anode and the other close to the cathode.

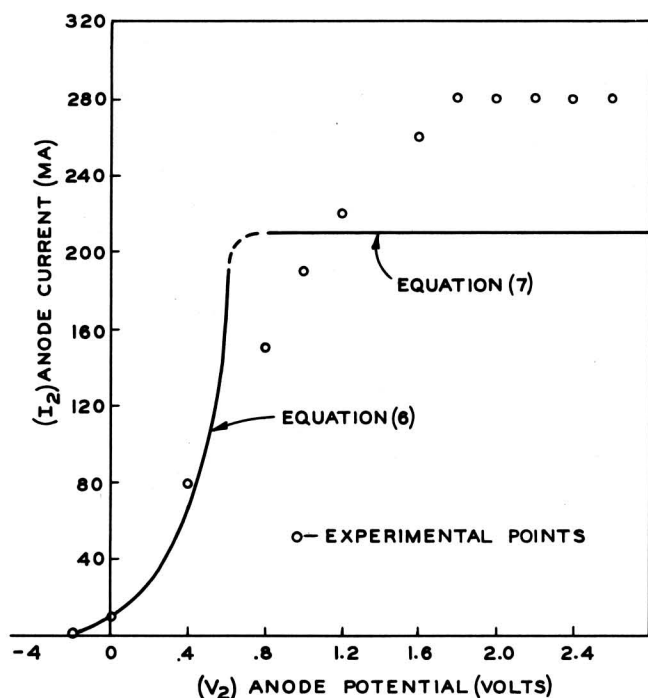


Fig. 16 - Comparison of computed anode current with experiment.

The values of the space-current densities used in equation (6) were determined by conventional probe techniques. The electron temperature was measured by the double-probe method² and was found to be close to the thermal temperature of the cathode. The potential drops across the plasma were measured by noting the change in floating potential between the two probes. This potential difference was found to be about 0.04 volt indicating a plasma resistance of about 2-ohm centimeters. This is

*See Appendix.

lower than the value predicted by Eq. (1) because of the density gradients in the plasma

The emission density of the 50-mil diameter oxide-coated cathode was determined by running this cathode, in conjunction with its anode, as a conventional gas diode and noting the value of anode current at which the discharge broke out of the "ball of fire" mode.³ This value of anode current is approximately one-half the total field-free emission of the cathode.

If the potential V_s is given a value of 0.95 volts, Eq. (6) includes the point 0.0 volts, 10 milliamperes. This value of potential seems reasonable and about what might be expected from contact potentials and a small drop in the plasma.

The curve representing Eq. (6) was terminated by the horizontal portion at the point where

$$I_2 = A_a j_{oa} \quad (7)$$

since Eq. (6) does not hold beyond here. The agreement between the two curves is fair and about as good as one might expect from this simple analysis. At least part of the deviation between the curves stems from a small cathode coating resistance.

Whereas the positive ion current has been neglected it will actually amount to several milliamperes when the anode is negative. This back current must be considered in certain applications such as in rectification where this current could result in accelerated gas clean-up as well as in premature inverse breakdown.

A comparison between the actual saturated anode current and that computed from Eq. (7), by probe measurements of plasma density, is displayed in Fig. 17. The deviation at low currents probably arises from the tendency of the positive ion sheath surrounding the probe to overlap the electron sheath adjacent to the anode for low plasma densities. The deviation at high currents stems from (1) the partial saturation of the cathode which causes the

³The "ball of fire" form of discharge is described by M. J. Druyvesteyn and F. M. Penning, "Electrical Discharges in Gases", *Rev. Mod. Phys.*, Vol. 12, p. 148; April, 1940.

actual anode current to drop, and (2) the fact that the measuring probe was about 2 millimeters from the anode surface and consequently measured a somewhat higher plasma density than that actually adjacent to the anode.*

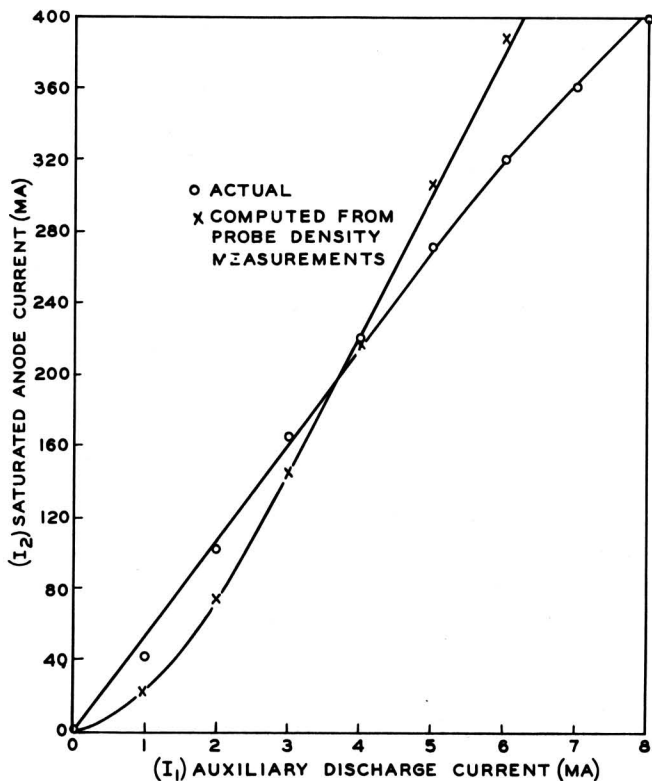


Fig. 17 - Comparison of saturated anode current with its computed value.

The relation between the saturated anode current and the auxiliary current, with the cathode emission as parameter, is shown in Fig. 18. This family of curves shows how the saturated anode current is first limited at the anode, as exemplified by the linear dependence of this current on the auxiliary current and hence on the plasma density, and then saturates at a value corresponding to the emission capability of the cathode. The values of cathode emission were measured in the same manner as before. The agreement between these values and the anode current along the horizontal portion of the curves is surprisingly good considering the usual vagaries of the emission from oxide-coated cathodes. Measurements were made as rapidly as possible to prevent changes in the cathode surface due to ion bombardment.

*The increase in plasma density with decreasing radial distance from the cathode is discussed in the Appendix.

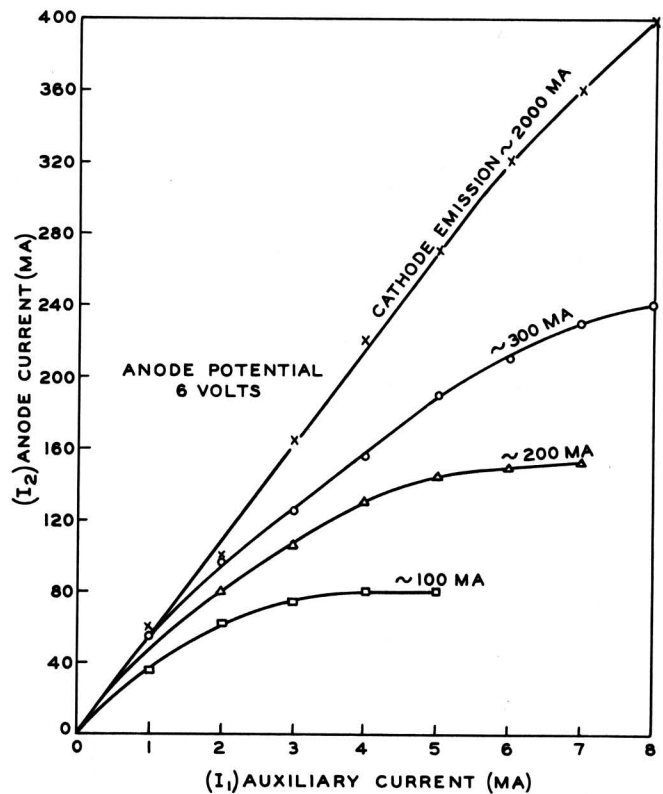


Fig. 18 - Relation between anode and auxiliary discharge currents with cathode emission as parameter.

Theoretically the departure from linearity should occur when the cathode-to-plasma potential V_k becomes zero. Then, from Eq. (6),

$$A_{kj_k} = A_{kj_{ok}} + A_{aj_{oa}}$$

$$\text{whence } \frac{A_{kj_k}}{I_2} = \frac{A_{kj_{ok}}}{A_{aj_{oa}}} + 1 \quad (7')$$

Since saturation occurs at the anode (along the linearly dependent portion of Fig. 19) it follows that the total random current flow through a cylindrical shell coaxial with the cathode must be greater than that through the anode sheath.**Then $A_{kj_{ok}} > A_{aj_{oa}}$. Substitution of this inequality into Eq.(7') yields $A_{kj_k} > 2I_2$. That is, for normal plasmatron operation the cathode emission should be at least twice the maximum saturated anode current demanded.

Eq. (7) also indicates that the anode current should be independent of cathode area when the tube is operating with anode satu-

**See Appendix.

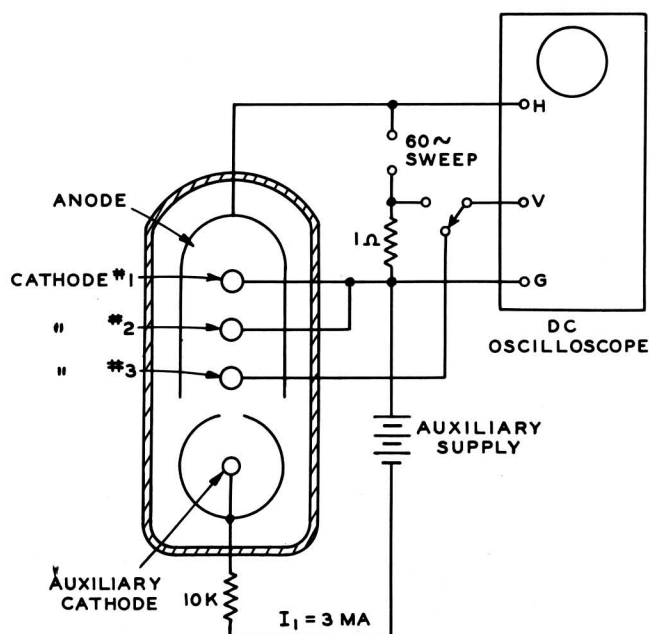


Fig. 19 - Circuit for investigating the behavior of plasma potential.

ration. This was tested by employing a tube with three separate main cathodes of equal area. This arrangement allowed the cathodes to be used separately or in various parallel combinations. The results are tabulated in Table I (a). It is seen that the anode current is essentially unaffected by cathode area. Part (b) of the same table shows the effects which occur when the cathode emission is temperature limited. Here, as was expected, the anode current is seen to be equal to the sum of the cathode emission.

To verify qualitatively the reality of the behavior of the plasma potential (as it has been portrayed) the arrangement of Fig. 19 was employed. (This same tube was used to provide the data of Table I). This arrangement enabled the floating potential V_f of cathode No. 3, acting as a probe, to be observed as the volt-ampere characteristic of the main cathode-anode circuit was swept at a 60-cycle rate. For these tests cathode No. 3 was made a strong emitter so that its potential was very close to that of the plasma. The curves in Fig. 20 (a) and (b) show the correspondence between the volt-ampere characteristic and the potential V_f which is essentially plasma potential. In the first case, where the cathode is a strong emitter, the plasma potential starts to rise with the anode current and stops rising when the anode

Table I

(a) Anode Saturation	
Cathode No.	Anode Current (ma)
1	300
2	240
3	200
1 and 2	280
1 and 3	260
2 and 3	240
1 and 2 and 3	260
(b) Cathode Saturation	
Cathode No.	Anode Current (ma)
1	(Negligible)
2	14
3	56
1 and 2	--
1 and 3	--
2 and 3	68
1 and 2 and 3	--

current saturates. This behavior is in accord with that predicted by the analysis. Furthermore, the magnitude of the change in plasma potential is such as to account for the change in the current leaving the cathode. Little can be said with respect to the absolute value of the plasma potential since the contact potentials are not known. However, in other experiments made under more ideal conditions where the contact differences of potential could be measured, it was found that the plasma potential was actually about 0.5 volts below that of the cathode. Also, the fact that the plasma electron temperature, measured in plasmas which are closely associated with copiously emitting cathodes, is generally very close to the temperature of the cathode is in itself a strong indication that such plasmas are below cathode potential. This temperature correspondence holds for oxide as well as pure metal cathodes.

In Fig. 20 (b), where the cathode is a weak emitter, we see that the plasma potential moves up linearly with the anode potential once the anode current has saturated. This is in accord with the analysis which predicts that most of the tube drop occurs near the cathode when the cathode is a poor emitter.

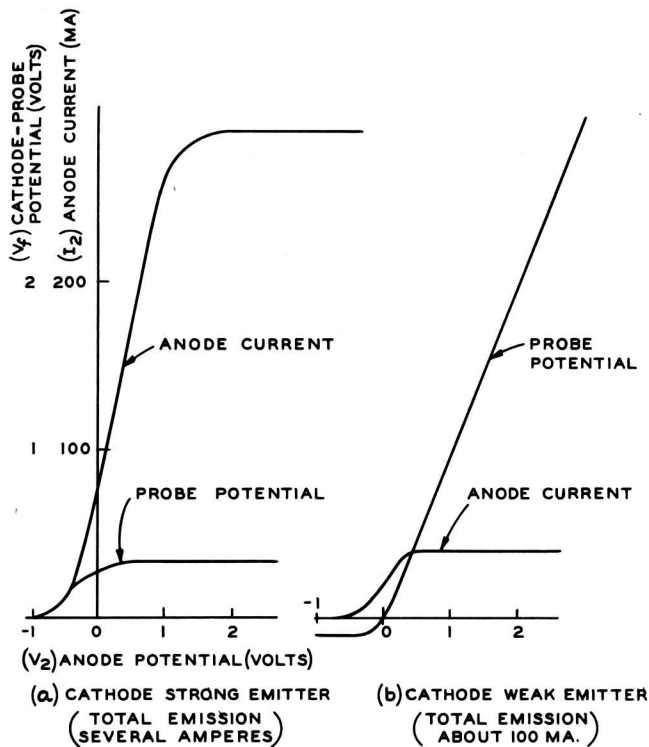


Fig. 20 - Relation between plasma potential and anode current

- (a) Cathode a strong emitter
(b) Cathode a weak emitter

In summary it can be said that our simple picture of plasmatron behavior is in good agreement with a diversity of experimental results.

There are conditions under which the cathode-plasma-anode system becomes unstable. Usually the only tendency towards instability that shows up in a helium-filled tube seems to occur when the system is operated with the cathode as an emitter of intermediate capabilities. Under these conditions probe measurements show that the plasma potential alternates between the distributions of Fig. 15 (a) and (b). When the instabilities give coherent oscillations these have a period corresponding to that of the Tonks-Langmuir ion oscillations.⁴

When the gas filling is one of the heavier gases, such as xenon, then the tube is quite likely to become unstable. The reason for this is not yet clearly understood. There are indications, however, that this difficulty arises from non-symmetrical plasma density distributions that are not appropriate to the current

densities that have to be carried at the various cross sections in a cylindrical-type geometry.* Non-symmetries in the plasma density are fostered by the fact that the ion generation is usually most intense in the region between the garrote and the main cathode in a tube type such as those already illustrated.

Plasma Generation and Loss**

The auxiliary discharge is the sole agent for generating the necessary plasma since the main anode current is not allowed to ionize in normal operation. In plasmatrons of the types already described it seems that the major part of the ionization can be ascribed to the ionizing collisions that the stream of electrons emerging from the aperture in the garrote makes upon neutral atoms.

The dependence of this type of ionization in helium upon electron energy is shown in Fig. 21.⁵ The dashed curve refers to the efficiency of ion generation as defined by the ion pairs generated per volt energy of the impinging electrons. The most copious generation occurs at $V = 100$ volts and the most efficient at $V = 55$ volts. At a gas pressure of p millimeters of mercury the differential ion current di_p arising from the ion generation, in a distance dx , by an electron current i_e is given approximately by

$$di_p = f(V) i_e \epsilon^{-x/\lambda'_e} dx$$

Here the ionization function $f(V)$, is to a first approximation, as displayed in Fig. 21, the factor ϵ^{-x/λ'_e} is the fraction of the original electron current i_e still able to ionize after traveling the distance x , and λ'_e is a distance comparable to the mean free

*See Appendix.

**The plasma density is largely determined by the ion supply since the copious thermionic supply and high mobility of the electrons allows them to accommodate readily to the density conditions imposed by the ions. Thus the term "ion" will often be used in place of the term "plasma" in this section.

⁴L. Tonks and I. Langmuir, OSCILLATIONS IN IONIZED GASES, *Phys. Review*, Vol. 33, pp. 195-210; Feb. 1929.

⁵M. Knoll, GASENTLADUNGSTABELLEN, J. Springer, Berlin, 1935, p. 66.

path of the electrons at the pressure p with regard to inelastic collisions.

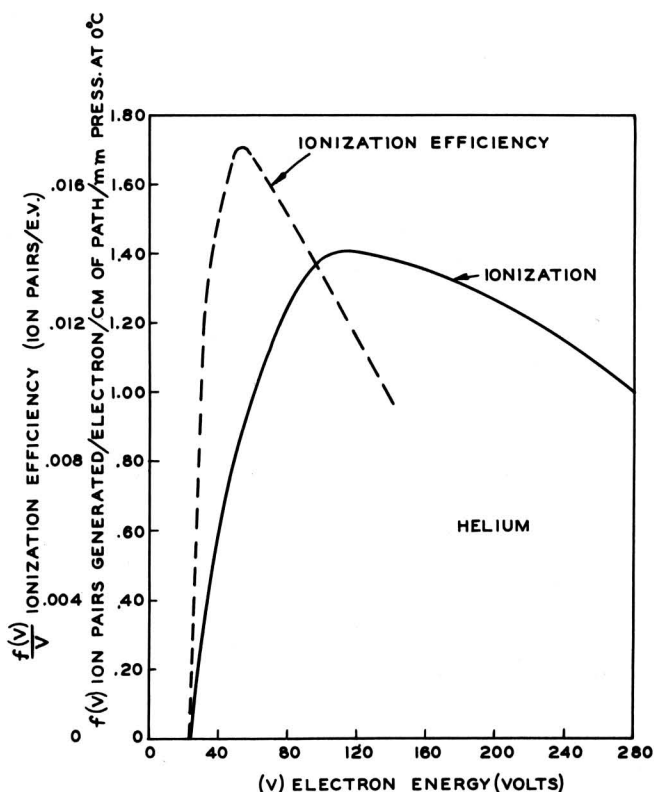


Fig. 21 - Relation between ion generation and electron energy.

Integration of the above equation over a distance d , large compared to λ'_e , yields

$$i_p = f(V) i_e \lambda'_e \quad (8)$$

Since the ionization function varies directly, and λ'_e inversely with pressure, Eq. (8) is independent of pressure. This equation represents the total ion current i_p generated in the region that the ionizing current i_e acts upon. The process by which the current i_p is lost from this region will now be investigated.

The volume recombination that takes place in the plasma is relatively negligible in the plasmatron so that the loss occurs principally by wall recombination. That is, the free electrons and ions in the plasma diffuse to the available bounding surfaces where they recombine. The travel of the free electrons and positive ions to the available surfaces occurs by an ambipolar diffusion process wherein ions and

electrons leave the plasma at equal rates. This process will result in a total rate of loss of ions from the plasma as accounted for by

$$\frac{dN}{dt} = -\frac{N}{\tau} \quad (9)$$

where N is the total number of ions in the plasma and τ is the plasma decay constant, in seconds, and is described by⁶

$$\tau = \frac{\Lambda^2}{D_a} \quad (10)$$

Here Λ is the characteristic diffusion path in centimeters and D_a is the ambipolar diffusion coefficient in square centimeters per second. The quantities N , τ , and Λ all refer to the lowest density mode of the plasma. The higher density modes have been neglected for the sake of simplicity since such an omission will not have any serious effect upon the approximate results desired in this investigation.

The application of these quantities to the plasmatron requires comment. In the direction parallel to the main cathode the usual ambipolar diffusion coefficient can be used because the total ion and electron currents arriving to the end micas are equal. However, in the direction normal to this, i.e., the cathode-anode direction, there usually is such a large disparity between the ion and electron currents that the usual value of the ambipolar coefficient is no longer valid.* This disparity stems from the small electric field in the plasma which serves to direct the electrons to the anode edge of the plasma and at the same time concentrate the positive ions toward the cathode. As the anode current and anode potential increase, a decreasing number of positive ions can leave the plasma at the anode. In the limit, when the anode current is saturated, the electron sheath at the anode prevents any ions from leaving at this boundary. Also, the potential barrier at the cathode prohibits ion loss at this point. Except for the loss to the end micas, the garrote, and a

⁶M. A. Biondi and S. C. Brown, "Measurements of Ambipolar Diffusion in Helium", *Phys. Rev.*, Vol. 75, pp. 1700-1705; June 1949.

*See Appendix.

very small amount of volume recombination, the positive ions are effectively trapped. Consequently, the values of Λ and D_a to be used in describing the plasmatron losses are generally not related to the vessel geometry or the mobility and diffusion coefficients in the manner described by Biondi and Brown.⁶ This added complication presents no special problem since the effective value of τ can easily be evaluated by pulsing the auxiliary discharge and noting the rate at which the saturated main anode current decays. It is felt that the value of τ so obtained is not materially different than that which holds sway in the tube during normal operating conditions, particularly since the electron temperature seems to be about the same in both cases.

By introducing the electron charge e into Eq. (9) the ion current i_p lost from plasma region is found to be

$$i_p = \frac{Ne}{\tau}$$

When Eq. (8) is introduced into this, there results:

$$f(V) \lambda_e' i_e = \frac{Ne}{\tau} \quad (11)$$

Probe studies of plasma density and the requirements upon the plasma density* indicate that N can be expressed in terms of the average plasma density n_{oa} adjacent to the anode, and the active tube volume v , by

$$N = \psi n_{oa} v$$

The factor ψ , which has a value of about 2.0, is independent of the anode current and arises from the greater plasma density in the cathode region. Combining Eqs. (2), (2'), and (7), Eq. (11) becomes

$$f(V) \lambda_e' i_1 = 0.4 \times 10^{-8} \frac{j_{oa} v}{\tau} \quad (12)$$

Here j_{oa} is expressed in milliamperes per

*Appendix.

square centimeter, v in cubic centimeters, the electron temperature is taken as $1000^\circ K$, and the ionizing current i_e has been replaced by its equivalent i_1 , the auxiliary discharge current expressed in milliamperes.

This equation, first of all, predicts that the anode current should be proportional to the ionization function $f(V)$.^{*} This prediction is borne out by the results shown in Fig. 22 where the crosses represent normalized values taken from Fig. 21. The auxiliary voltage was controlled by varying the garrote bias. The larger the bias, the greater the constricting effect at the aperture,⁷ and hence the larger the arc drop.^{**}

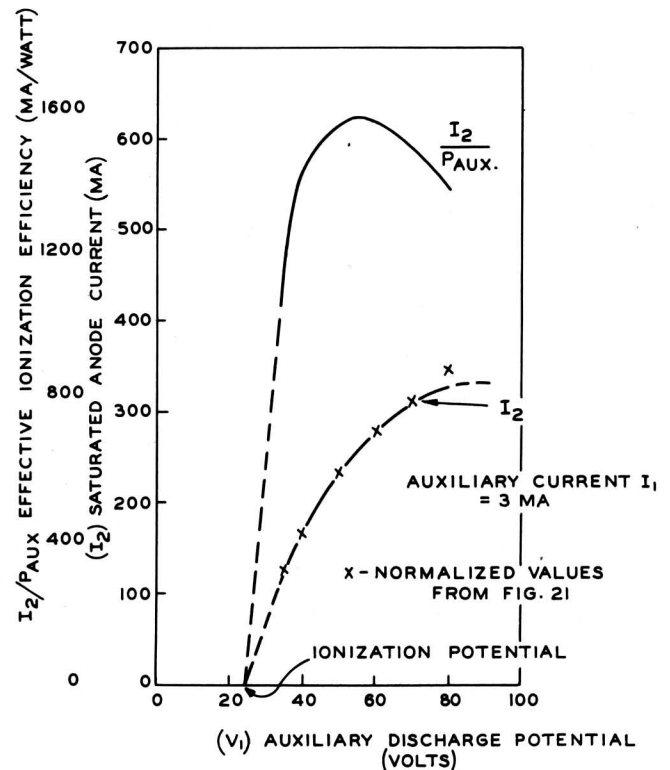


Fig. 22 - Relation between saturated anode current and auxiliary discharge potential.

*For simplicity the ionization mean free path for electrons was chosen for the value of λ_e . Actually, λ_e also depends upon exciting collisions and the probable loss of some of the electrons to the walls by elastic scattering. These effects would tend to keep λ_e relatively independent of V so that the anode current would closely follow $f(V)$.

⁷H. Fetz, "On the Control of a Mercury Arc by means of a Grid in the Plasma", *Ann. der Phys.* Vol. 37, pp. 1-40; January, 1940.

**Probe studies show that virtually all of the arc drop appears in the aperture.

Secondly, Eq. (12) indicates that the anode current should be proportional to the auxiliary current I_1 . The results in Figs. 4 and 17 bear adequate testimony to the validity of this conclusion.

Thirdly, Eq. (12) suggests that the current gain, as defined by the ratio of the saturated anode current to the auxiliary current, should be directly proportional to the decay constant τ . Both the qualitative and quantitative behavior shown in Fig. 23 confirm this very nicely. However, the unusually good quantitative results probably contain an element of fortuity which derives from the approximations introduced into the derivation of Eq. (12).

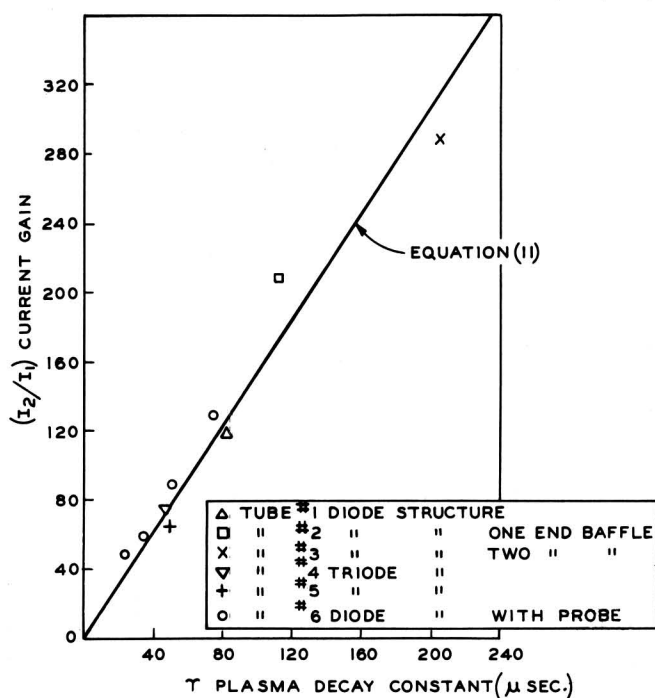


Fig. 23 - Relation between current gain and plasma decay constant.

In evaluating Eq. (12) the following values were used: $A_a = 8.5 \text{ cm}^2$, $v = 3.25 \text{ cm}^3$, $V = 60 \text{ volts}$, and $\lambda_e = 0.235^8 \text{ centimeters}$ at $p = 1 \text{ millimeter pressure}$. The tubes represented in Fig. 23 were identical with the one shown in Fig. 2 except for small geometrical differences in the main cathode-anode region which altered τ . For example, tube No. 3 had positive baffles over the end micas. These prevented ion losses to the micas and so altered τ .

⁸ Landolt-Bornstein, ZAHLENWERTE UND FUNKTIONEN AUS PHYSIK UND CHEMIE, J. Springer, Berlin, 1950.

It is instructive to consider the effective ionization efficiency curve shown in Fig. 22. Here the peak efficiency corresponds to 1.5 amperes of anode current for each watt in the auxiliary discharge. Operation under these conditions is several times as efficient as the operation of an ordinary hot cathode diode. To illustrate this point compare the total energy consumed in tube drops for a given anode current (1) using plasmatron operation and (2) using the same tube without the auxiliary discharge.

	(1) Plasmatron	(2) Diode
Anode current	0.26	0.26 a.
Anode voltage	2.0	27.0 v.
Auxiliary voltage	55.0	----
Auxiliary current	.003	----
Total power in tube drops	.69	7.0 w.

Now if the necessary auxiliary heater power of 1.0 watt (at the conservative rate of 20 milliamperes emission per watt heating power) is added, the plasmatron shows a power loss which is only one quarter that of the diode. Had the gas been xenon, which has an ionizing potential of about 11 volts, the saving would still be 50 per cent or more. Thus the use of the plasmatron principle in rectifier circuits, where efficiency is a consideration, appears attractive.

These results emphasize that the ordinary hot cathode gas diode operates at a disadvantage in that its anode potential is beset with the dual problem of pulling electrons through the tube as well as having to take care of the ionization requirements.

Any particular ion density can be put to the best use by taking advantage of the fact that for a given ion density the anode current is proportional to the anode area as shown in Eq. (7). By using various stratagems, such as finned anodes, the anode area can be increased several-fold without increasing the outside dimensions of the tube. When this is done, current gains of 300:1 are easily achieved in tubes such as those illustrated. If the previously mentioned trapping action is pushed to extremes, by extending the anode over the end

micas and garrote, even greater current gain can be obtained.*

In dealing with the frequency response of the device in the first or diode method of operation one is concerned with the time constants of plasma build-up and decay. The plasma build-up time is a function of how fast ions can be generated by the auxiliary discharge. This process, which occurs in the order of a microsecond, is so much faster than the decay time that it can be ignored. The decay of the plasma density will proceed largely by ambipolar diffusion according to the relation⁹

$$n = n_0 e^{-t/\tau} \quad (13)$$

from which Eq. (9) was derived. Here n is the ion density at a particular point in the tube at a time t , n_0 is the initial ion density at this point, and τ is the decay constant previously described. As might be expected the sine wave frequency response is inversely related to the decay constant and drops off at the expected frequency.

Grid Action

In the second mode of operation the saturated anode current is controlled by varying the cross-section of the plasma in the vicinity of the anode. This is accomplished by interposing a grid between the main cathode and anode (see Fig. 7). The anode characteristic with grid bias as a parameter is plotted in Fig. 9. When the grid is at a negative potential with respect to the plasma, its wires are surrounded by positive ion sheaths which serve as barriers through which electrons cannot flow. Thus, the anode current is made to depend

*The volume recombination loss should become important when the plasma density n_{0a} at the anode has a value given approximately by $n_{0a} = \frac{1}{2\alpha\tau}$ which is derived by equating the diffusion to the recombination loss. Using the value 1.7×10^{-8} , given by Biondi and Brown for the volume recombination coefficient α of helium, and 100 microseconds for τ the value of n_{0a} turns out to be 3×10^{11} . This corresponds to an anode current of about an ampere in these tubes, which is approximately the current at which indications of volume recombination becomes evident.

upon the thickness of the grid sheaths. This control of the anode current appears as a variation of the effective anode area A_a in Eq. (7). Actually, an increasingly negative grid bias is effective in reducing the anode current in still another fashion. The sheaths act as ion sinks whose effect is to reduce the plasma density in their neighborhood. As the sheaths expand the plasma density decreases correspondingly resulting in a further decrease of the saturated anode current. This second control mechanism may be considered analytically as a variation of the effective random current density j_{0a} in Eq. (7). Thus, the grid exerts control over the anode current through two cooperating mechanisms: (1) The variation of the effective collection area of the anode, and (2) the variation of the current density able to flow through this area.

The relative contributions of the A_a and j_{0a} variations have been estimated in the following fashion. From a measurement of the positive ion current to the grid when it was highly negative, a value for plasma density was obtained. Assuming that the plasma density is the same for all other values of grid bias, the sheath thickness as a function of grid bias was computed by the methods described by Malter and Webster.⁹ It was further assumed that A_a , and consequently the anode current, was proportional to the region between the grid wires not closed off by adjacent sheaths. The resultant anode current grid voltage characteristic is plotted in Fig. 24. Here the ordinate is plotted in terms of the current at zero bias. For comparison the experimental results are plotted on the same figure. The anode current was always maintained in a saturated condition. It is seen that the experimental characteristic is very nearly the square of the theoretical characteristic (indicated by crosses). This suggests that the variation in anode current is controlled about equally by the two mechanisms and that the effective anode area and the random electron current density are nearly linear functions of the grid sheath radius.

Efforts to use the grid itself as a probe for determining the plasma density in its vicinity as a function of its own negative bias did not yield the expected variation. This is

⁹L. Malter and W. M. Webster, "Rapid Determination of Gas Discharge Constants from Probe Data", *RCA Review*, Vol. 12, p. 191; June, 1951.

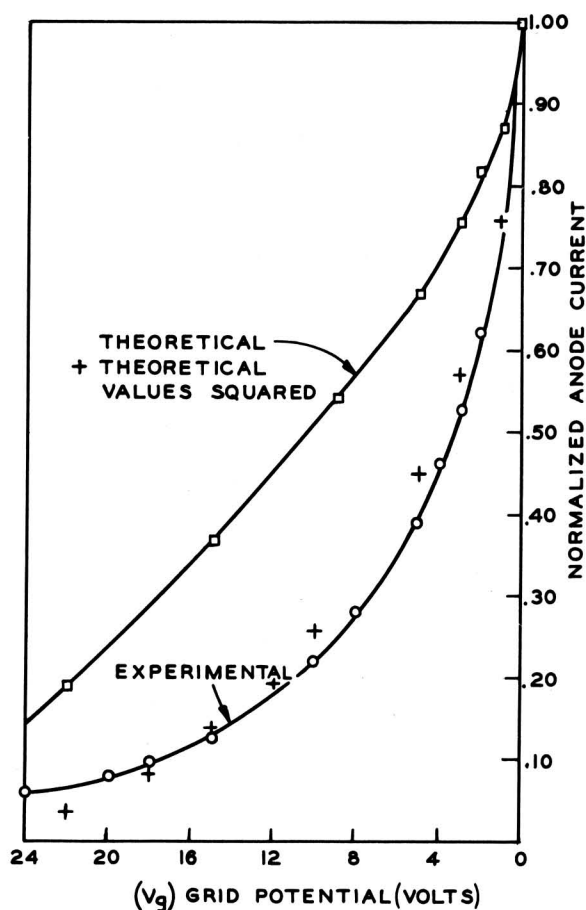


Fig. 24 - Comparison between theoretical and experimental grid control characteristic.

no doubt due to the marked variation of plasma density from the front to the rear of the grid sheath which produces a pear shaped sheath. This is evidenced by the appearance of the dark space surrounding the grid wires. As a consequence, plasma density determinations carried out on the basis of cylindrical sheaths (only these are readily amenable to analysis) are bound to yield erroneous results.

The similarity between the volt-ampere output characteristics of the diode and triode operation stems from the fact that the grid action affects the total quantity $A_{aj\ o a}$ of Eq. (7) just as the auxiliary discharge does. Comparison of Fig. 3 with Fig. 9 shows that a higher value of auxiliary current is required to give the same anode current in the triode as in the diode. This comes about because even at zero bias the grid wires act as ion sinks which reduce the plasma density adjacent to the anode.

The triode frequency response, plotted in

Fig. 10, is compounded of a complex combination of ion and electron movements in the grid-anode region. The falling off of response is a result of the finite time required to alter the plasma density in the grid-anode region. For example, if region is closed off from the main body of the plasma the residual plasma therein soon disappears by diffusing to the grid wires. When the sheaths are then retracted, a definite length of time, primarily determined by the slow-moving ions, is required for the plasma to be restored in the grid-anode region. This build-up time requires about 5 microseconds in these tubes, whereas the cut-off of the anode current by the grid sheaths occurs in a fraction of a microsecond.

It is interesting in the light of the above to point out why the thyatron grid, in contradistinction to the plasmatron grid, loses control after the onset of a discharge with its concomitant plasma formation. The loss of grid control, in the case of the thyatron, stems from the increase in ionization that necessarily accompanies the increase in the thickness of the grid sheath.⁷ As the grid sheaths reduce the span of the grid openings the anode current at first tends to decrease. This decrease, in the usual resistance-limited circuit, raises the anode potential making possible a higher rate of ion generation and hence a more dense grid-anode plasma. As a result of this greater plasma density the effect of the original grid sheath expansion is virtually cancelled and little net effect upon the anode current ensues. At very low gas pressures the rate of ion generation is less able to keep pace with the grid sheath expansion so that a certain amount of grid control can be achieved with grids that have small openings. At higher gas pressures, such as are normally used in commercial thyatrons, this is not usually the case. This entire matter has been studied very thoroughly by Fetzer and need not be elaborated upon at this point. The plasmatron escapes the difficulties of the thyatron by utilizing a plasma that is produced independently of the anode current.

General Behavior and Applications

While exhaustive life studies have not been carried out, it would seem that the plas-

matron would be at least as good in this respect as a comparable gas tube such as a thyatron. The presence of the retarding field, for positive ions, at the cathode precludes the possibility of trouble from disintegration of the cathode due to ion bombardment. This should also apply to the auxiliary cathode since the arc drop of the auxiliary discharge occurs across the aperture in the garrote and, in addition, there is also a small retarding field at the auxiliary cathode. It would seem that the low operating potentials normally required would not cause prohibitive gas clean up.

There is no reason to believe that the tube should behave any differently with respect to ambient temperatures than a thyatron filled with a noble gas should be relatively temperature insensitive.

Since the tube is a low voltage, high current, device, special attention must be given to the cathode. As regards overall efficiency, the cathode emission efficiency must be kept as high as possible and voltage drops in the cathode coating and interface must be kept to a minimum. It has been observed that such drops can add several volts to the po-

tential at which anode current saturation occurs.

Contact differences of potential between the cathode and anode are often noticeable in the plasmatron. During cathode activation the entire volt-ampere characteristic can be seen to drift toward lower anode potentials. This shift of the characteristic is presumed to be due to the decrease in the anode work function which follows from the deposit of evaporated cathode material.

In its present developmental stage the tube has been used in the laboratory for direct loudspeaker drive, motor control, switching, regulation, inversion, and low drop rectification.

Conclusions

A new electronic device, a continuously controllable hot cathode gas tube, has been described and its operation analyzed. This tube shows excellent promise for fulfilling the long-standing need for a device that will continuously control large currents at low voltages.


Edward O. Johnson


W. M. Webster


L. Malter

Appendix

It is instructive to make a simplified analysis of plasma conditions in a cylindrical geometry such as in Fig. 25. It is assumed that the charged particle densities are equal so that $n^+ = n^- = n$. This assumption seems justified on the basis of an analysis made on plane parallel structures where n^+ and n^- were not assumed equal. It cannot be expected to hold near plasma boundaries.

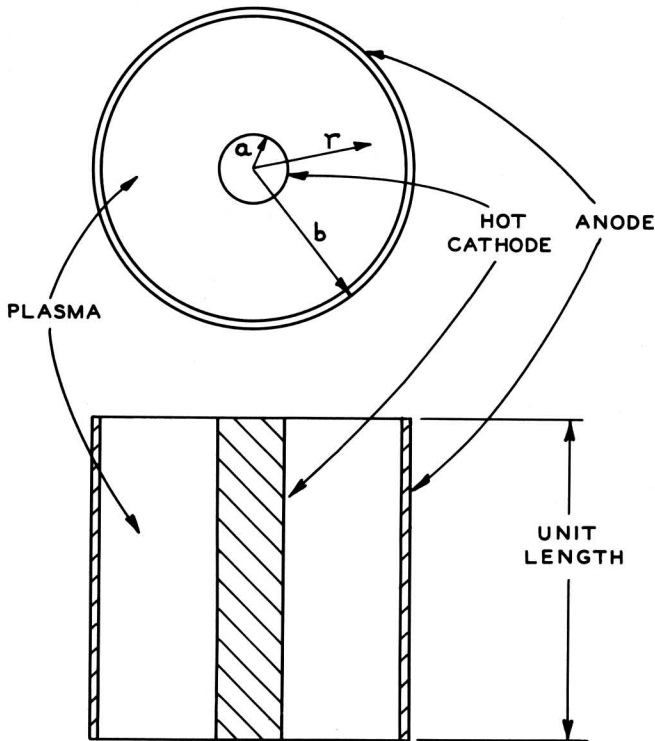


Fig. 25 - Section of plasmatron diode.

The electrons enter the plasma at the cathode with a density q_a^- and leave at the anode with a flow density aq_a^-/b . The positive ions are allowed to enter either at the anode or cathode with a flow density q_o^+ , or to be present and have no net drift velocity in a radial direction.

In addition to the current continuity relations and the above boundary conditions the flow equations

$$q^+ = nE\mu^+ - D^+ \frac{\partial n}{\partial r} \quad (1)$$

$$q^- = nE\mu^- - D^- \frac{\partial n}{\partial r} \quad (2)$$

must be satisfied. q^+ and q^- are the respective positive ion and electron particle flows, resp., μ^+ and μ^- are mobilities, D^+ and D^- the diffusion coefficients, n is the particle (plasma) density at the radius r , and E is the field.

From Eqs. (1) and (2) one obtains

$$q^+ = - \left[\frac{D^+\mu^- + D^-\mu^+}{\mu^- + P\mu^+} \right] \frac{dn}{dr} = - D'_a \frac{dn}{dr} \quad (3)$$

where D'_a is the modified ambipolar diffusion coefficient and $P = \pm q^-/q^+$. The positive sign refers to the case where the particle flows are in the same direction and the negative sign where the flow directions are opposed. By definition D'_a is the ambipolar diffusion coefficient D_a when $P = 1$. Since $\mu^- \gg \mu^+$, D'_a will not start to differ appreciably from D_a until the absolute value of P becomes greater than 20 or so. This is an interesting result since it indicates that diffusion conditions are still "ambipolar" even when there is a relatively large disparity between electron and positive ion flows to boundaries. However, when the flows differ by a factor of a 100 or more, as they do in the radial direction in the plasmatron, then conditions are far removed from ambipolar.

From Eqs. (1) and (2), the continuity relations, and the boundary conditions one obtains:

$$dn = - \frac{aq_a^-}{D_a} \left[\frac{\mu^+}{\mu^-} \pm \frac{r_o q_o^+}{aq_a^-} \right] \frac{dr}{r} \quad (4)$$

The positive sign refers to the case where the positive ions enter at the cathode and the negative sign to the case where they enter at the anode. In the first case $r_o = a$, and in the second $r_o = b$.

If n_b is the positive ion density adjacent to the anode, Eq. (4) becomes

$$n = n_b + \frac{aq_a^-}{D_a} \left[\frac{\mu^+}{\mu^-} \pm \frac{r_o q_o^+}{Aq_a^-} \right] \ln \frac{b}{r} \quad (5)$$

This shows that if the positive ions enter at

the cathode, remain essentially stationary (as they would for low rates of generation and loss), move in an axial direction, or enter at the anode at such a rate that the quantity in the bracket does not become negative, the plasma density will be greatest close to the cathode. If in Eq. (5), q_a^- is proportional to n_b and q_o^+/q_a^- remains approximately constant, then the density distribution function will be essentially independent of the anode current. Experiment indicates that such is the case. If q_a^- is not proportional to n_b , as would be the case if the anode current is not saturated, then Eq. (5) shows that the plasma density in the cathode region should increase with q_a^- . Also because fewer ions can run out at the anode the density in this region might be expected to increase somewhat. These conclusions are well borne out by the results of probe measurements in the anode and cathode regions of a plasmatron. Typical behavior, where the probe current was measured as the anode current was changed, is shown in Fig. 26. Plasma decay studies also show that the disappearance of positive ions is markedly lessened as the anode current approaches its saturation value.

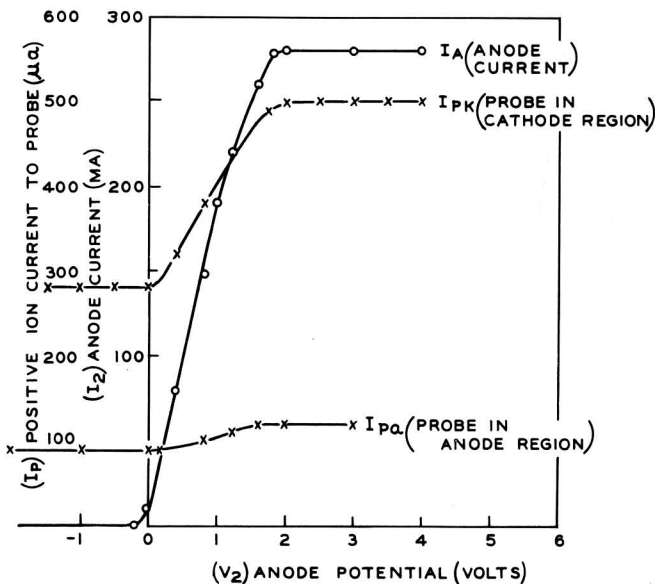


Fig. 26 - Effect of anode current and potential on plasma density.

In developing the expressions to describe the plasmatron operation, it has been assumed that the current carrying capacity of the plasma is a minimum at the anode, that is, that: $A_b j_b < A_r j_r < A_a j_a$. Here the A's refer to

the plasma cross-section area normal to a radius and the j 's to the electron space current densities at these cross-sections. The conditions necessary for this situation to exist can be found from Eq. (5). Thus all will be well if

$$n_b b < n r$$

or

$$n_b b < n_b r + \frac{a q_a^-}{D_a} \left[\frac{\mu^+}{\mu^-} \pm \frac{r_o q_o^+}{a q_a^-} \right] r \ln \frac{b}{r} \quad (6)$$

$$1 < \frac{r}{b} + \frac{a q_a^-}{b n_b D_a} \frac{\mu^+}{\mu^-} F r \ln \frac{b}{r}$$

$$F = \left[1 \pm \frac{r_o}{a} \frac{q_o^+}{q_a^-} \frac{\mu^-}{\mu^+} \right]$$

It is convenient to introduce the dimensionless factor F to account for the effect of the current ratio. The equation can be simplified further by the introduction of the relations

$$\frac{a}{b} q_a^- = q_b^-, \quad \frac{q_b^-}{n_b} = \frac{c^-}{4}, \quad \theta = \frac{T^-}{T^+}.$$

Here c^- is the average electron thermal velocity and the T 's refer to the particle temperature. If the classical expressions for the average thermal velocities, the electron mean free path L^- , and mobilities are used one obtains;

$$1 < \frac{r}{b} + \frac{4}{\pi} \frac{\theta}{1 + \theta} \frac{r}{L^-} F \ln \frac{b}{r}$$

or, approximately

$$1 < \frac{r}{b} + \frac{r}{L^-} F \ln \frac{b}{r} \quad (7)$$

From Eq. (7) it is seen that the necessary conditions for normal plasmatron operation, wherein plasma saturation occurs at the anode and not elsewhere, can be met when the ratio a/b is not too small, when the pressure is such that L^- is not too large, and when the ions are injected close to the cathode so that F tends to be large. Qualitative observations bear out these conclusions. In fact, when instabilities in operation do occur the behavior of the plasma potential strongly suggests that the point of plasma saturation alternates between the cathode and anode regions indicating that Eq. (7) is not being continuously satisfied.